

Supporting Information for

Single-Point-Mutation Detection in RNA extracts using Gold Nanoparticles Modified with Hydrophobic Molecular Beacons.

Alfonso Latorre,[†] Christian Posch,[‡] Yolanda Garcimartín,[†] Susana Ortiz-Urda,^{*‡} Álvaro Somoza^{*†}

[†] Instituto Madrileño de Estudios Avanzados en Nanociencia (IMDEA Nanociencia), Cantoblanco, 28049 Madrid, Spain & CNB-CSIC-IMDEA Nanociencia Associated Unit "Unidad de Nanobioteología. Spain

[‡]Department of Dermatology, University of California San Francisco, USA.

Table of contents	1
Synthesis of modified CPG	1
Synthesis and MALDI data of Oligonucleotides	4
Synthesis and functionalization of gold nanoparticles	5
RNA Extracts	6
Detection experiments	7
Using oligonucleotides as targets	7
Using RNA extracts	24
Hydrodynamic size of particles	29
NMR spectra	30

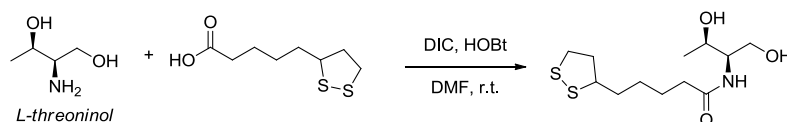
Synthesis of modified CPG

General Experimental Methods:

Reagents were purchased from Aldrich and used without further purification. Thin layer chromatography was carried out using Silica Gel 60 F254 plates. Column chromatography was performed using Silica Gel (60 Å, 230 x 400 mesh). All NMR spectra were recorded on Bruker

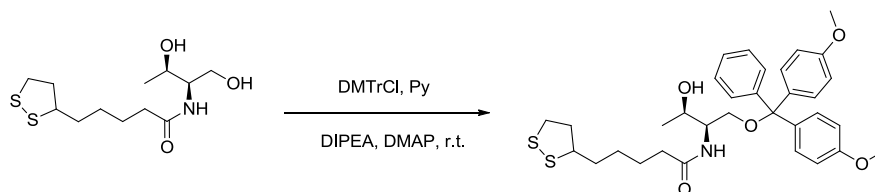
300 MHz instrument as solutions in the deuterated solvent indicated, and the chemical shifts are reported in parts per million (ppm). Coupling constants are reported in hertz (Hz).

5-[(3S)-1,2-dithiolan-3-yl]-N-[(1R,2S)-2-hydroxy-1-(hydroxymethyl)propyl]pentanamide (1).



To a solution of (*R*)-(+)-1,2-dithiolane-3-pentanoic acid (3.301 mmol, 680 mg, 1.2 eq.) in DMF (0.5 M) at room temperature, *N*-hydroxybenzotriazole (3.027 mmol, 409 mg, 1.1 eq.) and diisopropylcarbodiimide (3.026 mmol, 468 μ l, 1.1 eq.) were added. After stirring the mixture 10 min. *L*-threoninol (2.752 mmol, 289 mg, 1 eq.) was added. The resulting mixture was stirred overnight and then quenched by the addition of methanol. The solvent was evaporated under vacuum and the residue purified by flash chromatography 20:1 (CH_2Cl_2 : MeOH) to yield 660 mg as a pale yellow oil (82%). **¹H-NMR (300 MHz, CDCl_3):** δ 6.26 (d, J = 6.7 Hz, 1H), 4.17 (d, J = 6.2 Hz, 1H), 3.95 – 3.71 (m, 3H), 3.58 (dt, J = 13.1, 6.5 Hz, 1H), 3.48 (s, 1H), 3.26 – 3.04 (m, 2H), 2.46 (td, J = 12.4, 6.4 Hz, 1H), 2.27 (t, J = 7.4 Hz, 2H), 1.91 (dq, J = 13.7, 6.9 Hz, 1H), 1.80 – 1.60 (m, 5H), 1.57 – 1.41 (m, 2H), 1.19 (d, J = 6.4 Hz, 3H). **¹³C-NMR (75 MHz, CDCl_3):** δ 174.1 (C), 68.7(CH), 65.0(CH_2), 56.4(CH), 54.7(CH), 40.3(CH_2), 38.5(CH_2), 36.5(CH_2), 34.6(CH_2), 28.8(CH_2), 25.5(CH_2), 20.6(CH_3). **HR-MS (ESI):** m/z calculated for $\text{C}_{12}\text{H}_{24}\text{NO}_3\text{S}_2$ 294.1192 [$\text{M}+\text{H}$]⁺, found 294.1186.

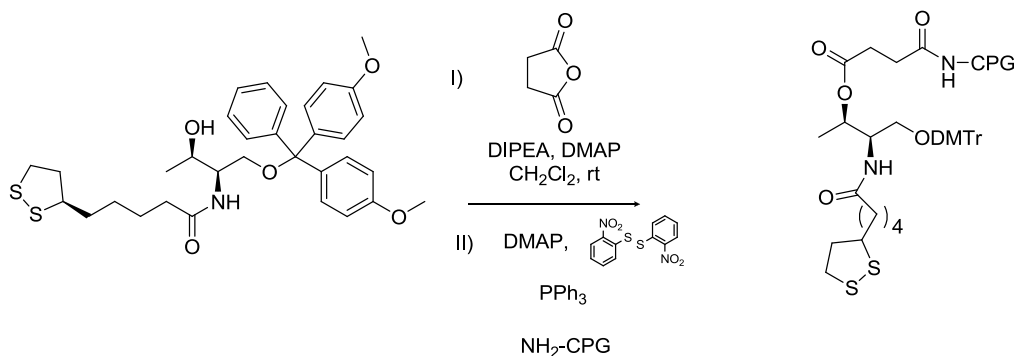
N-[(1R,2S)-1-{[bis(4-methoxyphenyl)(phenyl)methoxy]methyl}-2-hydroxypropyl]-5-[(3S)-1,2-dithiolan-3-yl]pentanamide (2).



To a solution of the corresponding diol (0.682 mmol, 200 mg, 1 eq.) in pyridine (0.2 M) at 0°C, diisopropylethylamine (1.023 mmol, 179 μ l, 1.5 eq), 4,4'-dimethoxytrityl chloride (0.819 mmol, 277 mg, 1.2 eq) and dimethylaminopyridine (catalytic amount) were added. After 15 min. the mixture was allowed to reach room temperature. The mixture was stirred overnight and then quenched by the addition of methanol. The solvent was evaporated under vacuum and the residue purified by flash chromatography 1:2 (hexane: EtOAc) to yield 270 mg as a white to light yellow foam (66%). **¹H-NMR (300 MHz, CDCl_3):** δ 7.28 (m, 9H), 6.83 (d, J = 8.8 Hz, 4H), 6.03 (d, J = 8.7 Hz, 1H), 4.10 (m, 1H), 3.93 (dd, J = 8.4, 2.5 Hz, 1H), 3.79 (s, 6H), 3.62 – 3.48 (m, 1H), 3.41 (dd, J = 9.6, 4.3 Hz, 1H), 3.29 (dd, J = 9.6, 3.5 Hz, 1H), 3.23 – 3.05 (m, 3H), 2.44 (td, J = 12.4, 6.4 Hz, 1H), 2.23 (t, J = 7.3 Hz, 2H), 1.90 (td, J = 13.7, 6.9 Hz, 1H), 1.76 – 1.62 (m, 4H), 1.56 – 1.41 (m, 2H), 1.12 (d, J = 6.4 Hz, 3H). **¹³C-NMR (75 MHz, CDCl_3):** δ 173.0 (C), 158.6 (2C) (C), 144.3 (C), 135.5 (C), 135.3 (C), 129.9 (2C) (CH), 129.8 (2C) (CH), 127.9 (2C) (CH), 127.8 (2C) (CH), 127.0(CH), 113.3 (4C) (CH_3), 86.7, 68.6(CH), 65.2(CH_2), 60.3, 56.3(CH), 55.2(CH), 53.3(CH),

40.2(CH₂), 38.4(CH₂), 36.5(CH₂), 34.6(CH₂), 28.9(CH₂), 25.5(CH₂), 19.9(CH₃). **HR-MS (ESI):** *m/z* calculated for C₃₃H₄₁NNaO₅S₂ 618.2324 [M+Na]⁺, found 618.2296.

CPG Functionalization (two steps)



I

To a solution of **2** (0.084 mmol, 50 mg, 1 eq) in anhydrous dichloromethane (0.2 M) succinic anhydride (0.109 mmol, 10.9 mg, 1.3 eq), diisopropylethylamine (0.118 mmol, 20.5 μ l, 1.4 eq) dimethylaminopyridine (catalytic amount) were added. The solution was stirred for 16 h at room temperature. The solution was washed with water and extracted with dichloromethane. The organic layer was dried over MgSO₄, filtered and evaporated under vacuum to yield yellowish oil.

II

To a solution of DMAP (0.126 mmol, 15.4 mg, 1.5 eq) in acetonitrile (60 mM) the product obtained in the step II was added (0.084 mmol, 58.3 mg, 1 eq). After mixing it well in vortex, the solution was added to a solution of 2,2'-dithiobis-(5-nitropyridine) (0.126 mmol, 39.0 mg, 1.5 eq) in anhydrous CH₂Cl₂ (300 μ l). The solution was mixed well and added to triphenyl phosphine (0.126 mmol, 33.0 mg, 1.5 eq). The mixture was vortexed till all reagents were dissolved giving rise to a reddish solution, which was added to 500 mg of CPG (500 Å). After 2h at room temperature, the solution was removed and the CPG washed with methanol (3 x 20 ml) and dry acetonitrile (3 x 20 ml). Once the CPG was dry, 2 ml of a 1:1 mixture of the capping reagents (CAP A: 600 μ l pyridine, 500 μ l dry THF, 400 μ l acetic anhydride; CAP B: 1 ml dry THF, 400 μ l 1-methylimidazole) was added. After 20 min at room temperature, the CPG was washed with dry acetonitrile (6 x 20 ml) and dried well.

The CPG loading was calculated by detrytylation of the sample as follow: 10 mg of CPG were treated with 5 ml of detrytylation solution (3 ml of perchloric acid and 2 ml of ethanol) for 1 hour. Then 500 μ l of the mixture were dissolved in 2 ml of the detrytylation solution and absorbance was measured at 498 nm. Functionalization (F) was determined by Lambert-Beer law using a extinction coefficient of $7 \times 10^4 \text{ M}^{-1} \text{ cm}^{-1}$:

$$F = (\text{ABS} \times V) / (\epsilon \times g) = M / g$$

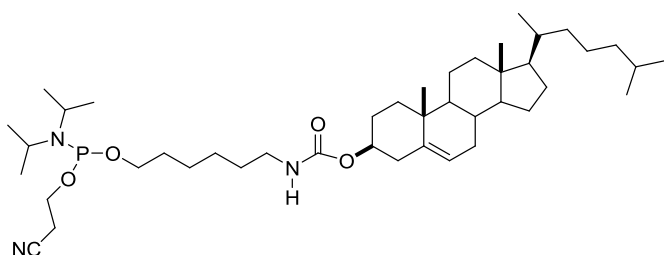
The loading of the modified CPG as prepared was 183 $\mu\text{M/g}$

Synthesis and MALDI data of Oligonucleotides

Oligonucleotides were prepared using a MerMade4 DNA Synthesizer using phosphoramidites (Link Technologies). DNA oligonucleotides were prepared at 1 μ Mol scale. After solid-phase synthesis, the solid support was transferred to a screw-cap glass vial and incubated at 55 °C for 4 h with 2 mL of ammonia solution (33%). After the vial was cooled on ice the supernatant was transferred by pipet to microcentrifuge tubes and the solid support and vial were rinsed with water. The combined solutions were evaporated to dryness using a evaporating centrifuge.

The samples were purified by polyacrylamide gel electrophoresis 20% and the oligonucleotides were eluted from gel fractions using an elutrap system. The solutions were desalted using a NAP-10 column and concentrated in an evaporating centrifuge.

Cholesterol modification (Chole) was incorporated using commercial available phosphoramidites (Link Technologies).



Dithiolane modification was incorporated using the modified CPG described above.

SEQUENCES

Entry	Name	Sequence
1	KRAS-WT-Chole	5'-Chole-AGCAAGACGCCACCAGCTCCACTTGCTAAAAA-Dithiolane-3'
2	KRAS-MUT-Chole	5'-Chole-AGCAAGACGCCACAAGCTCCACTTGCTAAAAA-Dithiolane-3'
3	KRAS-WT-Target	5'-TGGAGCTGGTGGCGT-3'
4	KRAS-MUT-Target	5'-TGGAGCTTGTGGCGT-3'
5	GNAQ-WT-Chole	5'-Chole-CCGTCTGACCTTTGGCCCCGACGGAAAAA -Dithiolane-3'
6	GNAQ-MUT-Chole	5'-Chole-CCGTCTGACCTTGGGCCCGACGGAAAAA-Dithiolane-3'
7	GNAQ-WT-Target	5'-GGGGGCCAAAGGTCA-3'
8	GNAQ-MUT-Target	5'-GGGGGCCAAAGGTCA-3'
9	RP-WT-Chole	5'-Chole-CTCCCCGTGGCGCCAGTTGGGAGAAAAA- Dithiolane-3'
10	RP-MUT-Chole	5'-Chole-CTCCCCGTGGCACCAGTTGGGAGAAAAA -Dithiolane-3'
11	RP-WT-Target	5'-CAACTGGCGCCACGG -3'
12	RP-Mut-Target	5'- CAACTGGTGCCACGG -3'
13	RP-MUT-Control	5'- CTCCCCGTGGCACCAGTTGGGAGAAAAA -Dithiolane-3'

Table S1. Sequences prepared in this work

MALDI

Entry	Name	Calc Mass	Found
1	KRAS-WT-Chole	10687.3	10674.9
2	KRAS-MUT-Chole	10711.3	10702.9
3	KRAS-WT-Target	4680.1	4677.1
4	KRAS-MUT-Target	4655	4651.4
5	GNAQ-WT-Chole	10084.8	10078.3
6	GNAQ-MUT-Chole	10109.8	10116.7
7	GNAQ-WT-Target	4667.1	4655
8	GNAQ-MUT-Target	4643.1	4631.01
9	RP-WT-Chole	9571.42	9565.5
10	RP-MUT-Chole	9555.42	9534.5
11	RP-WT-Target	4563.0	4551.1
12	RP-MUT-Target	4578.0	4568.6
13	RP-MUT-Control	8962.6	8973.3

Table S2. Maldi data of the sequences prepared

Maldi data was obtained at the Proteomic facility of the National Center for Biotechnology (CNB-CSIC) & at IMDEA Nanociencia using a Voyager DE Pro.

Synthesis and functionalization of gold nanoparticles

Gold Nanoparticles.

Gold Nanoparticles were prepared by the citrate reduction method.^[1]

A solution of HAuCl₄ (34.3 mg) in H₂O (101 mL) was heated up to reach boiling temperature then a solution of sodium citrate (119.4 mg) in H₂O (10.1 mL) was added quickly. The solution was stirred for 10 min and then the removed from the heating source and stirred overnight at room temperature. The reddish solution was filtered and stored at 4 C.

A UV/Vis spectrum of AuNPs showed the absorption inflection point at 520 nm, which was defined as the peak value to produce a diameter of 13 nm. This result was consistent with the observation from the high-resolution TEM image, in which a uniform size distribution of about 13 nm in diameter was observed. The concentration of AuNPs was determined using the Lambert-Beer law and the extinction coefficient of $2.7 \times 10^8 \text{ M}^{-1} \text{ cm}^{-1}$ at 520 nm.

[1] Ambrosi, A.; Castañeda, M. T.; Killard, A. J.; Smyth, M. R.; Alegret, S.; Merkoçi, A. *Anal. Chem.* **2007**, *79*, 5232–40.

Functionalization of Gold nanoparticles with oligonucleotides.

Gold nanoparticles were incubated with oligonucleotides (1, 2, 5, 6, 9, 10 and 13) overnight in a 0.3M NaCl buffer. The samples were purified by centrifugation, the supernatants were removed and the particles dissolved in water. This process was repeated 3 times.

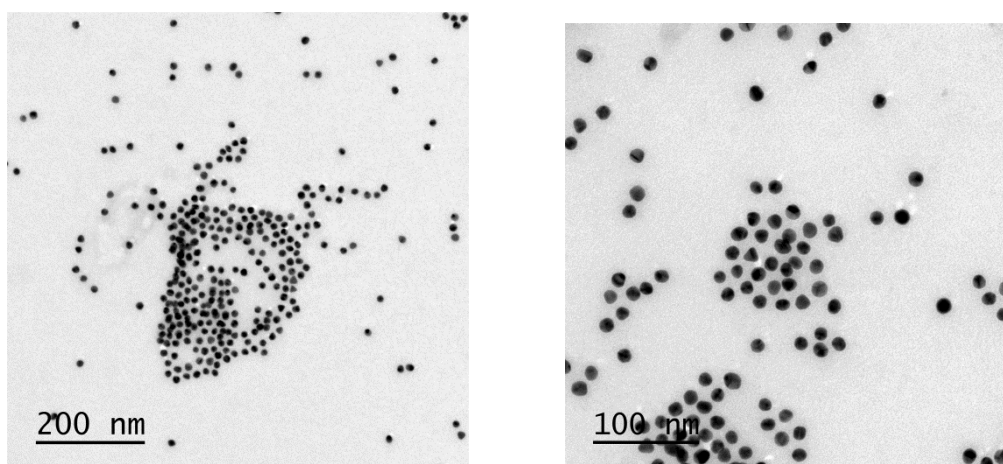


Figure S1 . TEM images of modified gold nanoparticles.

RNA Extracts

In this work we have used total RNA extracts from cell lines and tissue of mice. The required samples were obtained as follow:

Animal Tissue

Total RNA extracts from tissue (liver) were generated from 6-8 weeks old female Pde6b^{rd10}/Pde6b^{rd10} mice carrying a germ line, missense rd10 mutation in exon 13 of the Pde6b gene. Animals were euthanized by CO₂ asphyxiation and cervical dislocation. Liver tissue was collected under sterile conditions and flash frozen in liquid nitrogen. Frozen tissue was crushed, lysed with QIAzol Lysis Reagent (Qiagen, 79306), homogenized and subject to total RNA extraction with miRNeasy Mini Kit (Quiagen, 219004) following the manufacturer's instructions. All mouse studies were approved by the UCSF Institutional Animal Care and Use Committee.

Cell culture

Human melanoma cell lines OMM1.3, and C918 were available in Ortiz's lab at the University of California San Francisco. Cells were maintained in RPMI 1640 media supplemented with 10% FBS and grown at 37°C under 5% CO₂ until they reached 80-90% confluency. Cells were lysed with QIAzol Lysis Reagent (Qiagen, 79306) and total RNA was extracted with the miRNeasy Mini Kit (Quiagen, 219004) following the manufacturer's instructions.

Detection experiments

Using oligonucleotides as targets.

KRAS target sequence

Gold nanoparticles (50 μL , 13 nM) modified with oligonucleotides (1 or 2) were incubated with PBS (100 μL) and the target sequence (3 or 4) (5 μL , at the required concentration: 1 μM , 100 nM) during 4 h.

GNAQ Target sequence

Gold nanoparticles (50 μL , 13 nM) modified with oligonucleotides (5 or 6) were incubated with PBS (100 μL), NaCl (5M, 5 μL) and the target sequence (7 or 8) (5 μL , at the required concentration: 1 μM , 100 nM or 10 nM) during 16 h.

RP Target sequence

Gold nanoparticles (50 μL , 13 nM) modified with oligonucleotides (9 and 10) were incubated with PBS (50 μL), H₂O (50 μL) and the target sequence (11 or 12) (5 μL , at the required concentration: 1 μM , 100 nM or 10 nM) during 16 h.

KRAS Sensor.

Targeting WT KRAS

The nanoparticles designed to detect the WT KRAS gene were aggregated in the presence of the oligonucleotide sequence that matches the sequence in the nanoparticle (blue). The aggregation leads to a decrease in the plasmon band of gold nanoparticles at 530 nm. The aggregation was less intense in the presence of the oligonucleotide with the mutated KRAS sequence (green) or a scramble sequence (red).

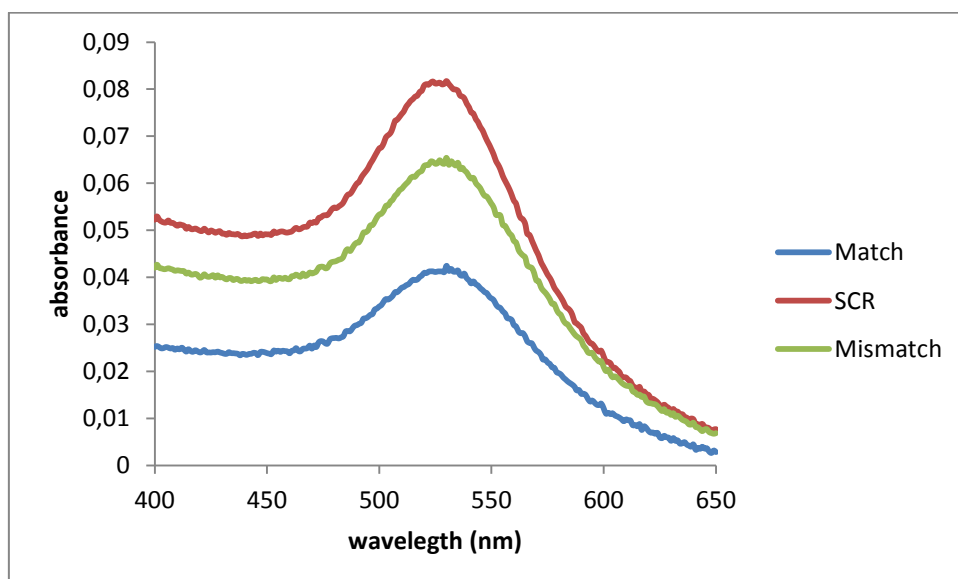


Figure S2. UV-Vis spectra of modified nanoparticles designed to detect the WT KRAS gene in the presence of the matched (blue), mismatched (green) and scramble (red) oligonucleotide sequences at 32 nM. There is a significant decrease in absorbance where the complementary sequence is present (Match). On the other hand, when there is a mismatched or scramble sequence the absorbance is higher

In this experiment the following sequences were employed:

Match: KRAS-WT-Target

SCR: RP-MUT-Target

Mismatch: KRAS-MUT-Target

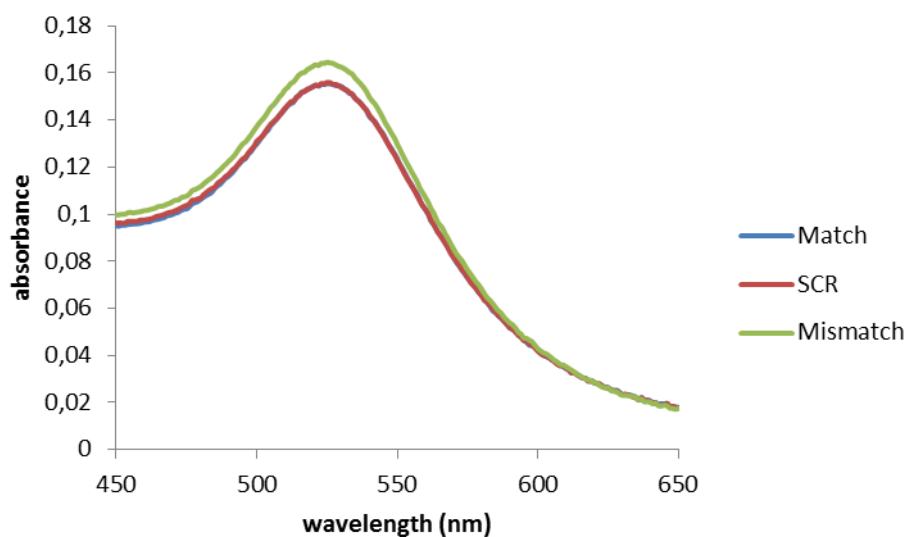


Figure S3. UV-Vis spectra of modified nanoparticles designed to detect the WT KRAS gene in the presence of the matched (blue), mismatched (green) and scramble (red) oligonucleotide sequences at 3.2 nM. There is not selectivity at this concentration.

In this experiment the following sequences were employed:

Match: KRAS-WT-Target

SCR: RP-MUT-Target

Mismatch: KRAS-MUT-Target

Targeting mutated KRAS

The nanoparticles designed to detect the mutated KRAS gene were aggregated in the presence of the oligonucleotide sequence that matches the sequence in the nanoparticle (blue). The aggregation leads to a decrease in the plasmon band of gold nanoparticles at 530 nm. The aggregation was less intense in the presence of the oligonucleotide with the WT KRAS sequence (green) or a scramble sequence (red).

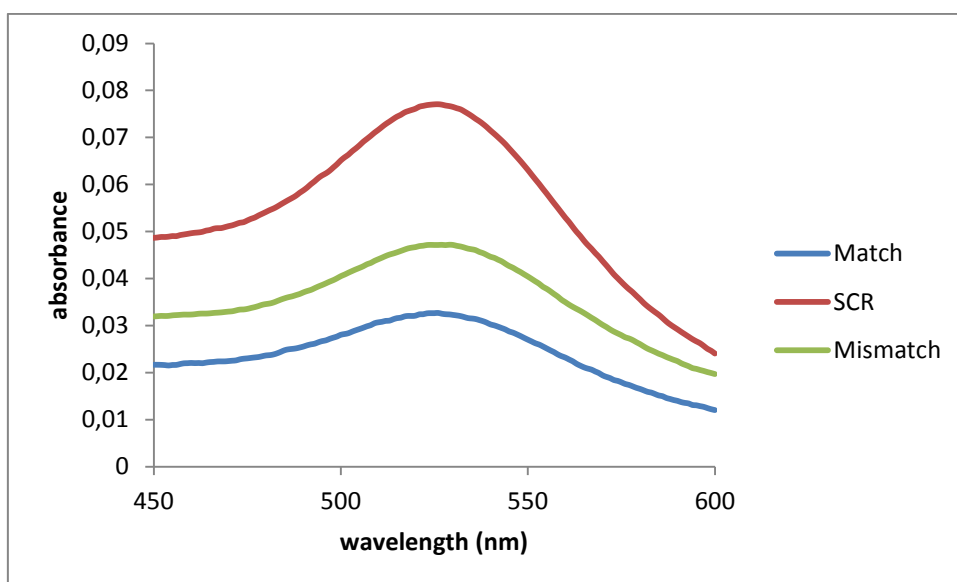


Figure S4. UV-Vis spectra of modified nanoparticles designed to detect the KRAS mutation in the presence of the matched (blue), mismatched (green) and scramble (red) oligonucleotide sequences at 32 nM. There is a significant decrease in absorbance where the complementary sequence is present (Match). On the other hand, when there is a mismatched or scramble sequence the absorbance is higher

In this experiment the following sequences were employed:

Match: KRAS-MUT-Target

SCR: RP-MUT-Target

Mismatch: KRAS-WT-Target

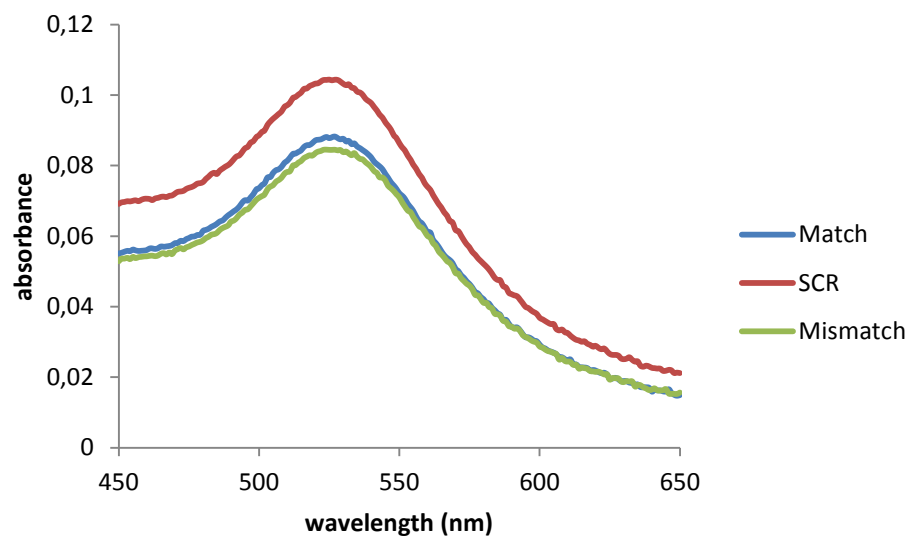


Figure S5. UV-Vis spectra of modified nanoparticles designed to detect the KRAS mutation in the presence of the matched (blue), mismatched (green) and scramble (red) oligonucleotide sequences at 3.2 nM. There is not selectivity at this concentration.

In this experiment the following sequences were employed:

Match: KRAS-MUT-Target

SCR: RP-MUT-Target

Mismatch: KRAS-WT-Target

GNAQ Sensor

Targeting the WT GNAQ

The nanoparticles designed to detect the WT GNAQ gene were aggregated in the presence of the oligonucleotide sequence that matches the sequence in the nanoparticle (blue). The aggregation leads to a decrease in the plasmon band of gold nanoparticles at 530 nm. The aggregation was less intense in the presence of the oligonucleotide with the mutated GNAQ sequence (green) or a scramble sequence (red).

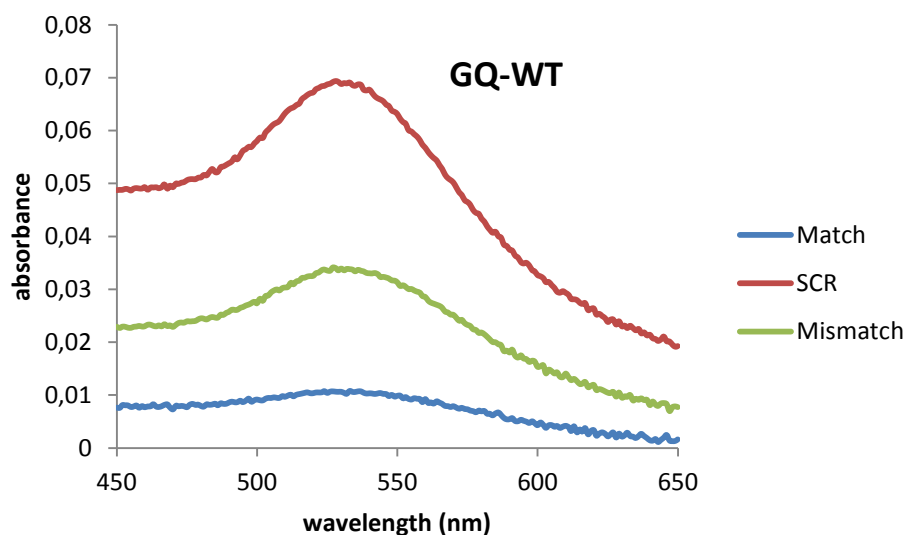


Figure S6. UV-Vis spectra of modified nanoparticles designed to detect the WT GNAQ gene in the presence of the matched (blue), mismatched (green) and scramble (red) oligonucleotide sequences at 32 nM. There is a significant decrease in absorbance where the complementary sequence is present (Match). On the other hand, when there is a mismatched or scramble sequence the absorbance is higher.

In this experiment the following sequences were employed:

Match: GNAQ-WT-Target

SCR: RP-MUT-Target

Mismatch: GNAQ-MUT-Target

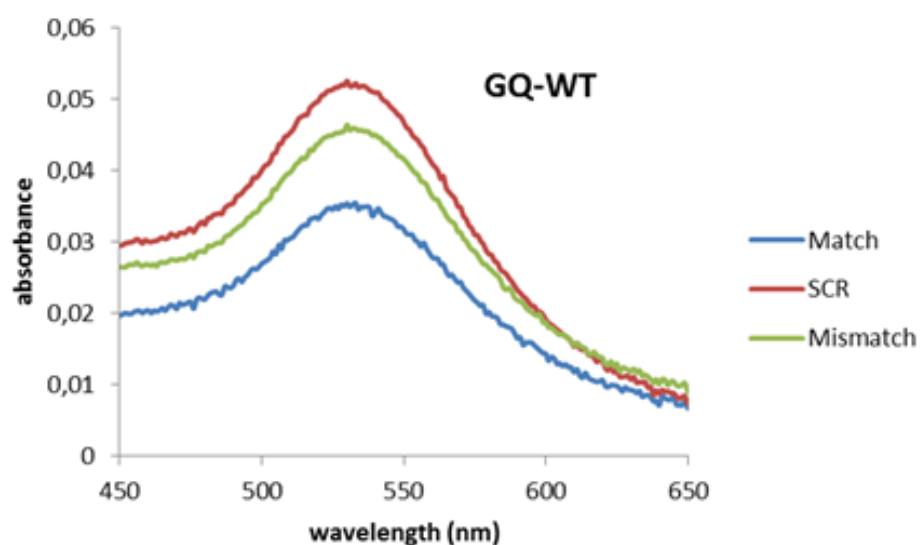


Figure S7. UV-Vis spectra of modified nanoparticles designed to detect the WT GNAQ gene in the presence of the matched (blue), mismatched (green) and scramble (red) oligonucleotide sequences at 3.2 nM. There is a significant decrease in absorbance where the complementary sequence is present (Match). On the other hand, when there is a mismatched or scramble sequence the absorbance is higher.

In this experiment the following sequences were employed:

Match: GNAQ-WT-Target

SCR: RP-MUT-Target

Mismatch: GNAQ-MUT-Target

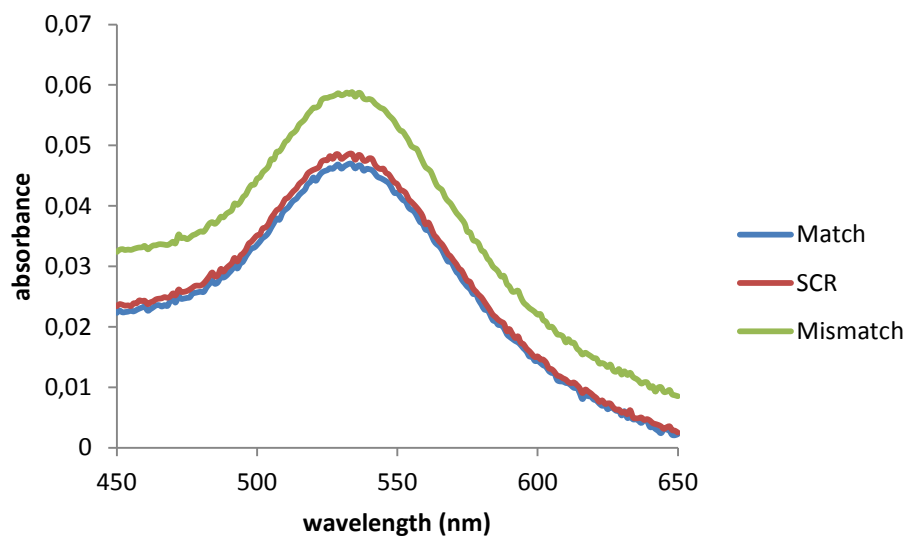


Figure S8. UV-Vis spectra of modified nanoparticles designed to detect the WT GNAQ gene in the presence of the matched (blue), mismatched (green) and scramble (red) oligonucleotide sequences at 322 pM. There is not selectivity at this concentration.

In this experiment the following sequences were employed:

Match: GNAQ-WT-Target

SCR: RP-MUT-Target

Mismatch: GNAQ-MUT-Target

Targeting the Mutated GNAQ

The nanoparticles designed to detect the mutated GNAQ gene were aggregated in the presence of the oligonucleotide sequence that matches the sequence in the nanoparticle (blue). The aggregation leads to a decrease in the plasmon band of gold nanoparticles at 530 nm. The aggregation was less intense in the presence of the oligonucleotide with the mutated GNAQ sequence (green) or a scramble sequence (red).

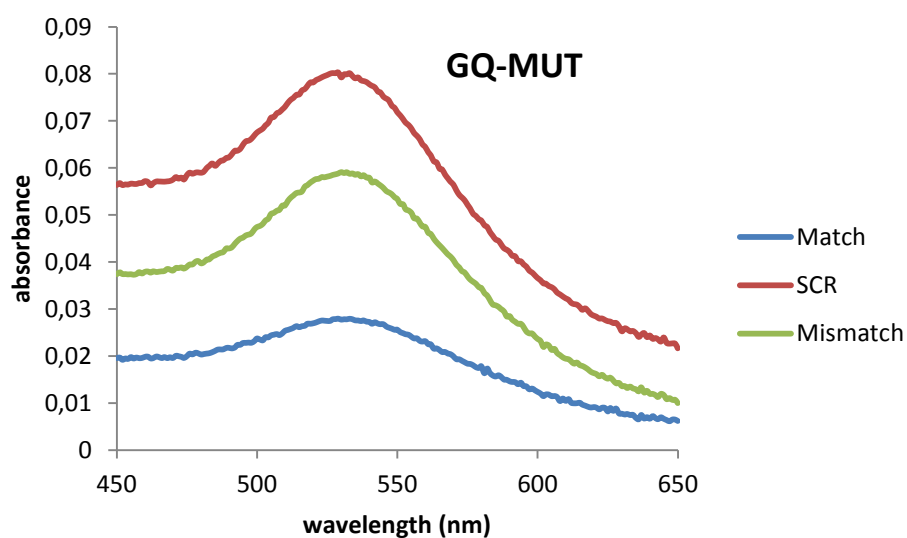


Figure S9. UV-Vis spectra of modified nanoparticles designed to detect the mutated GNAQ gene in the presence of the matched (blue), mismatched (green) and scramble (red) oligonucleotide sequences at 32 nM. There is a significant decrease in absorbance where the complementary sequence is present (Match). On the other hand, when there is a mismatched or scramble sequence the absorbance is higher.

In this experiment the following sequences were employed:

Match: GNAQ-MUT-Target

SCR: RP-MUT-Target

Mismatch: GNAQ-WT-Target

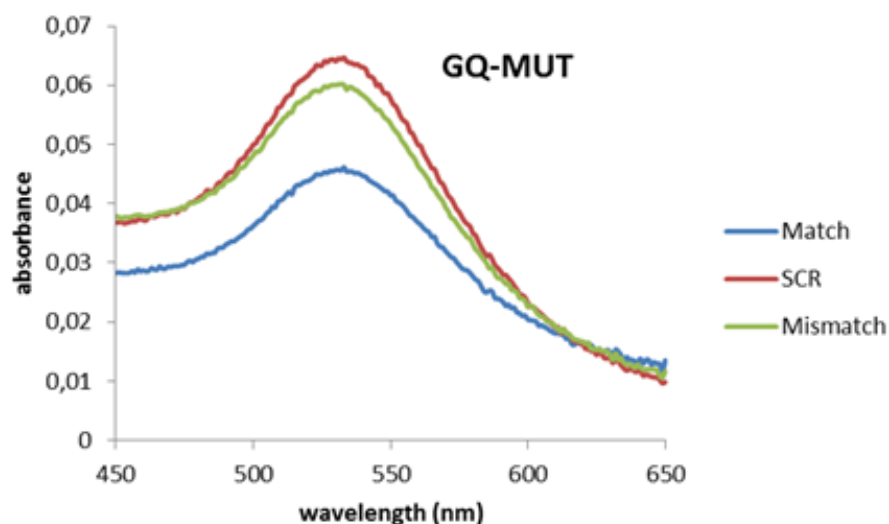


Figure S10. UV-Vis spectra of modified nanoparticles designed to detect the mutated GNAQ gene in the presence of the matched (blue), mismatched (green) and scramble (red) oligonucleotide sequences at 3.2 nM. There is a significant decrease in absorbance where the complementary sequence is present (Match). On the other hand, when there is a mismatched or scramble sequence the absorbance is higher.

In this experiment the following sequences were employed:

Match: GNAQ-MUT-Target

SCR: RP-MUT-Target

Mismatch: GNAQ-WT-Target

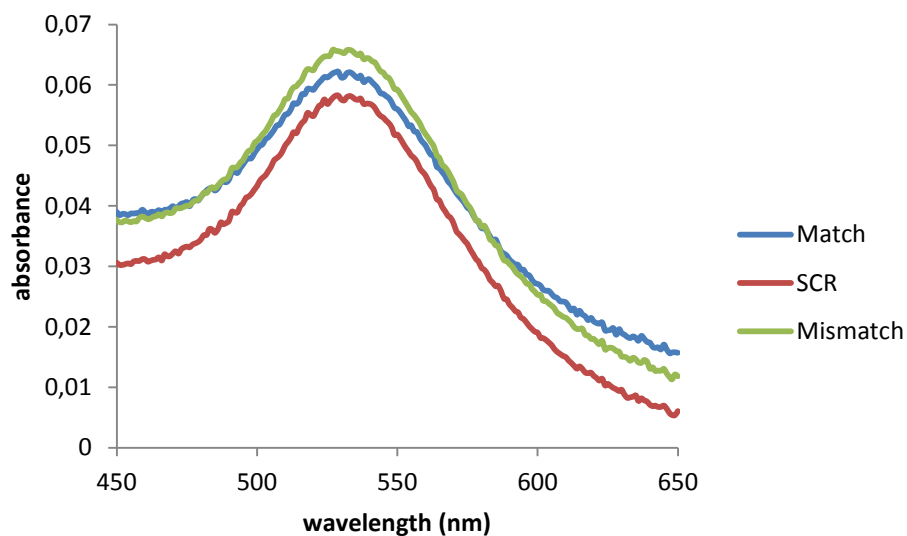


Figure S11. UV-Vis spectra of modified nanoparticles designed to detect the mutated GNAQ gene in the presence of the matched (blue), mismatched (green) and scramble (red) oligonucleotide sequences at 322 pM. There is not selectivity at this concentration.

In this experiment the following sequences were employed:

Match: GNAQ-MUT-Target

SCR: RP-MUT-Target

Mismatch: GNAQ-WT-Target

RP Sensor

Targeting the WT PDE6B gene

The nanoparticles designed to detect the WT PDE6B gene were aggregated in the presence of the oligonucleotide sequence that mimics the PDE6B gene (blue and green). The aggregation leads to a decrease in the plasmon band of gold nanoparticles at 530 nm. The aggregation was less intense in the presence of the oligonucleotide with the scramble sequence (red).

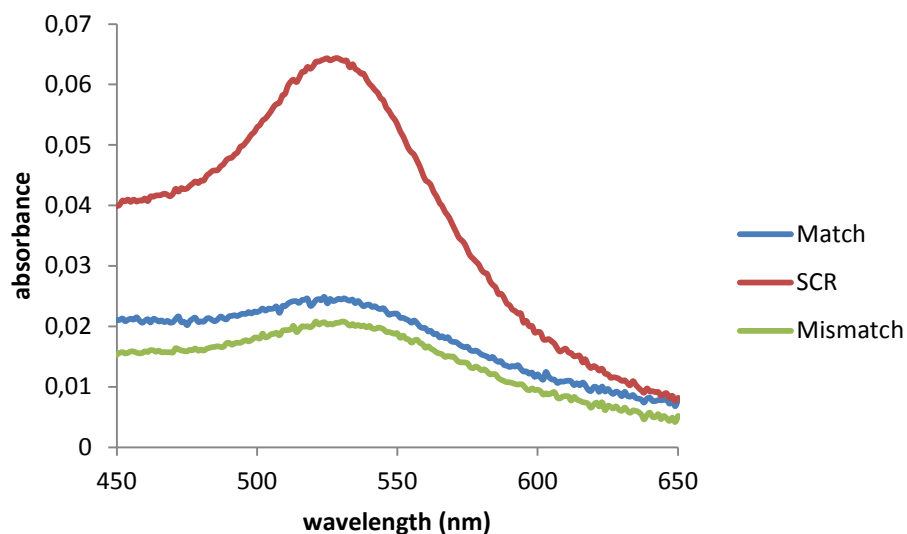


Figure S12. UV-Vis spectra of modified nanoparticles designed to detect the WT PDE6B gene in the presence of the matched (blue), mismatched (green) and scramble (red) oligonucleotide sequences at 32 nM. There is a decrease in absorbance where the gene is present (Match and Mismatch) compared with the scramble sequence.

In this experiment the following sequences were employed:

Match: RP-WT-Target

SCR: GNAQ-MUT-Target

Mismatch: RP-MUT-Target

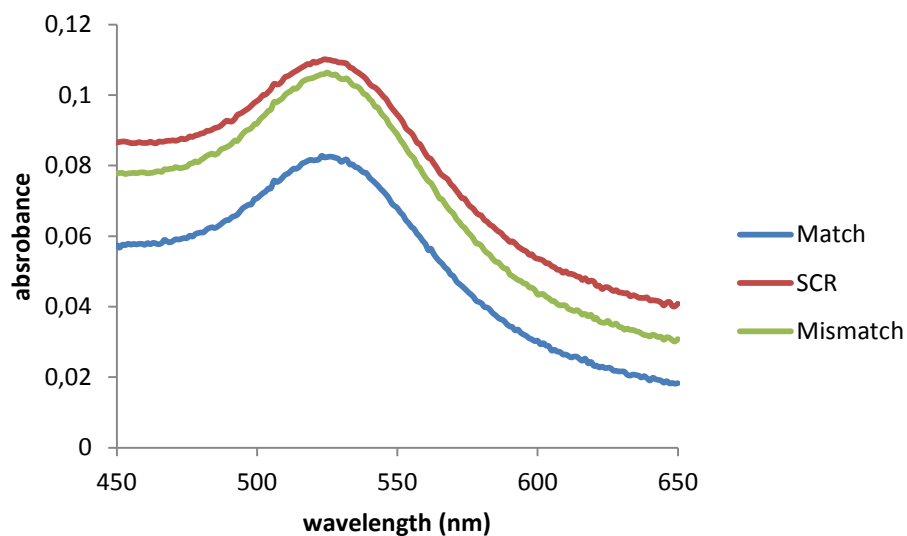


Figure S13. UV-Vis spectra of modified nanoparticles designed to detect the WT PDE6B gene in the presence of the matched (blue), mismatched (green) and scramble (red) oligonucleotide sequences at 3.2 nM. There is a decrease in absorbance where the gene is present (Match and Mismatch) compared with the scramble sequence.

In this experiment the following sequences were employed:

Match: RP-WT-Target

SCR: GNAQ-MUT-Target

Mismatch: RP-MUT-Target

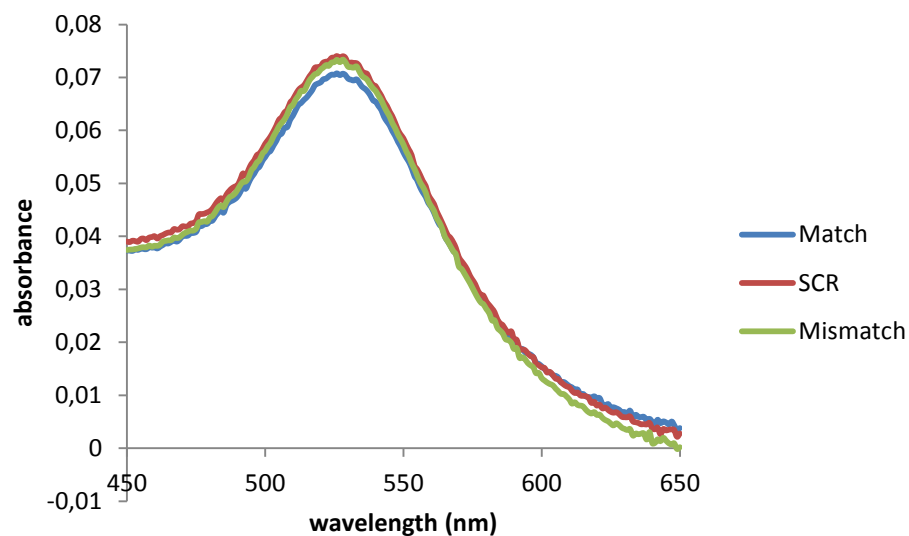


Figure S14. UV-Vis spectra of modified nanoparticles designed to detect the WT PDE6B gene in the presence of the matched (blue), mismatched (green) and scramble (red) oligonucleotide sequences at 322 pM. There is not selectivity at this concentration.

In this experiment the following sequences were employed:

Match: RP-WT-Target

SCR: GNAQ-MUT-Target

Mismatch: RP-MUT-Target

Targeting Mutated PDE6B gene

The nanoparticles designed to detect the mutated PDE6B gene were aggregated in the presence of the oligonucleotide sequence that matches the sequence in the nanoparticle (blue). The aggregation leads to a decrease in the plasmon band of gold nanoparticles at 530 nm. The aggregation was less intense in the presence of the oligonucleotide with the WT PDE6B sequence (green) or a scramble sequence (red).

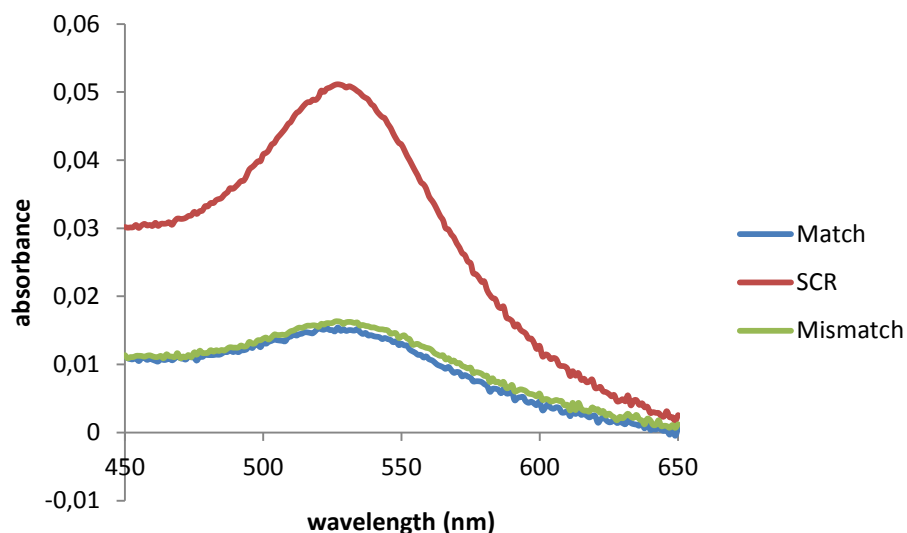


Figure S15. UV-Vis spectra of modified nanoparticles designed to detect the PDE6B mutation in the presence of the match (blue), mismatched (green) and scramble (red) oligonucleotide sequences at 32 nM. There is a significant decrease in absorbance where the complementary sequence is present (match). On the other hand, when there is a mismatched or scramble sequence the absorbance is higher.

In this experiment the following sequences were employed:

Match: RP-MUT-Target

SCR: GNAQ-MUT-Target

Mismatch: RP-WT-Target

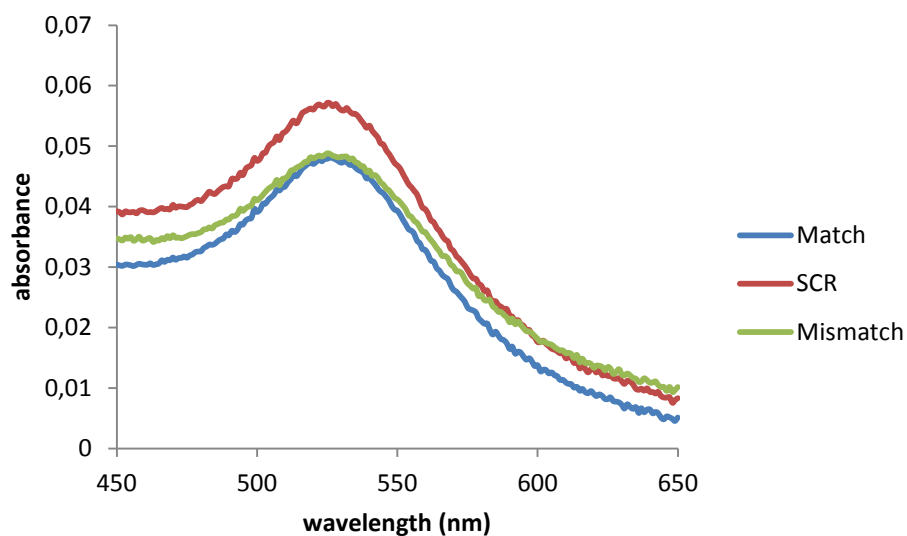


Figure S16. UV-Vis spectra of modified nanoparticles designed to detect the PDE6B mutation in the presence of the match (blue), mismatched (green) and scramble (red) oligonucleotide sequences at 3.2 nM. There is a significant decrease in absorbance where the complementary sequence is present (match). On the other hand, when there is a mismatched or scramble sequence the absorbance is higher.

In this experiment the following sequences were employed:

Match: RP-MUT-Target

SCR: GNAQ-MUT-Target

Mismatch: RP-WT-Target

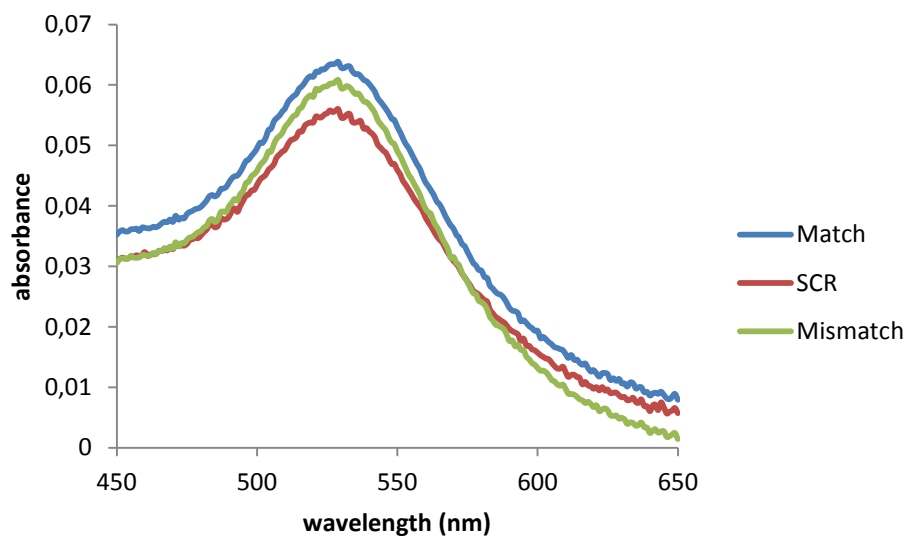


Figure S17. UV-Vis spectra of modified nanoparticles designed to detect the PDE6B mutation in the presence of the match (blue), mismatched (green) and scramble (red) oligonucleotide sequences at 322 pM. There is not selectivity at this concentration.

In this experiment the following sequences were employed:

Match: RP-MUT-Target

SCR: GNAQ-MUT-Target

Mismatch: RP-WT-Target

Targeting Mutated PDE6B gene with a control nanoparticle (without Cholesterol group).

We prepared a nanoparticle to detect the mutated PDE6B gene, but in this case we did not introduce a cholesterol group at the end of the oligonucleotide, as in the previous cases. Using the same conditions no aggregation was observed. This result highlights the key role of the hydrophobic cholesterol group in the sensor.

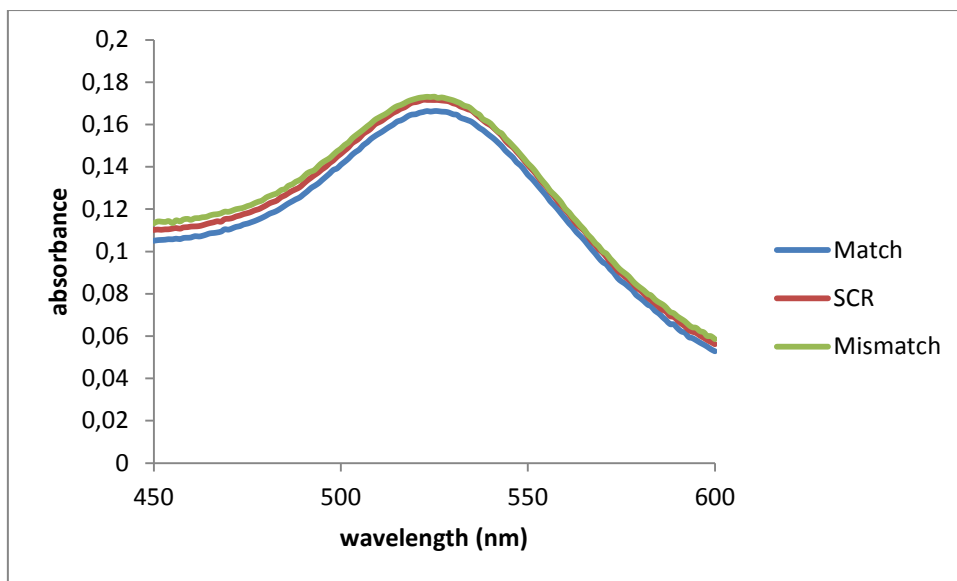


Figure S18. UV-Vis spectra of modified nanoparticles without the cholesterol modification designed to detect the RP mutation in the presence of the match (blue), mismatched (green) and scramble (red) oligonucleotide sequences at 3.2 nM. There is not a significant decrease in absorbance, therefore the presence of the cholesterol moiety is key to have an effective sensor.

In this experiment the following sequences were employed:

Match: RP-MUT-Target

SCR: GNAQ-MUT-Target

Mismatch: RP-WT-Target

Using RNA extracts

Total RNA extracts were obtained using standard procedures from mouse liver that express mutated RP gene, and the following cell lines C918 and OMM1.3. Stock solutions of RNA were prepared at 170 ng/ μ L and 85 ng/ μ L

Detection of GNAQ gene from RNA extracts.

Gold nanoparticles modified with oligonucleotides 5 or 6 (50 μ L) were incubated with PBS (95 μ L), NaCl (5M, 10 μ L) and total RNA extracts (15 μ L) obtained from 1) a cell line that express the wild-type gene (C918), 2) mouse liver extracts that does not contain the gene (RP) and 3) a cell line that express the mutated gene (OMM1.3). After 16 h the samples were analyzed using a UV-vis spectrometer or a microplate reader (Synergy H4, Biotek)

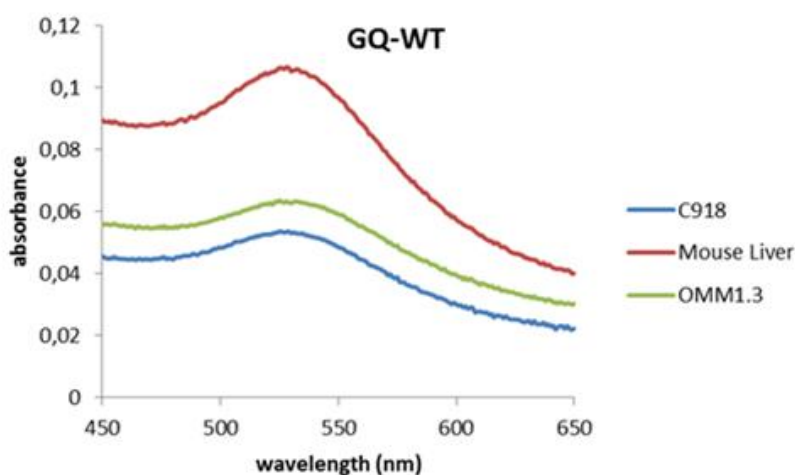


Figure S19. UV-Vis spectra of modified AuNPs after incubation with the total mRNA extracts (5.5 ng/ μ L) of different cell lines. C918 expresses wild type GNAQ, OMM1.3 expresses mutated GNAQ and mRNA from mouse liver that do not contain the GNAQ gene. The nanoparticles are designed to detect the wt GNAQ gene present in the C918 cell line.

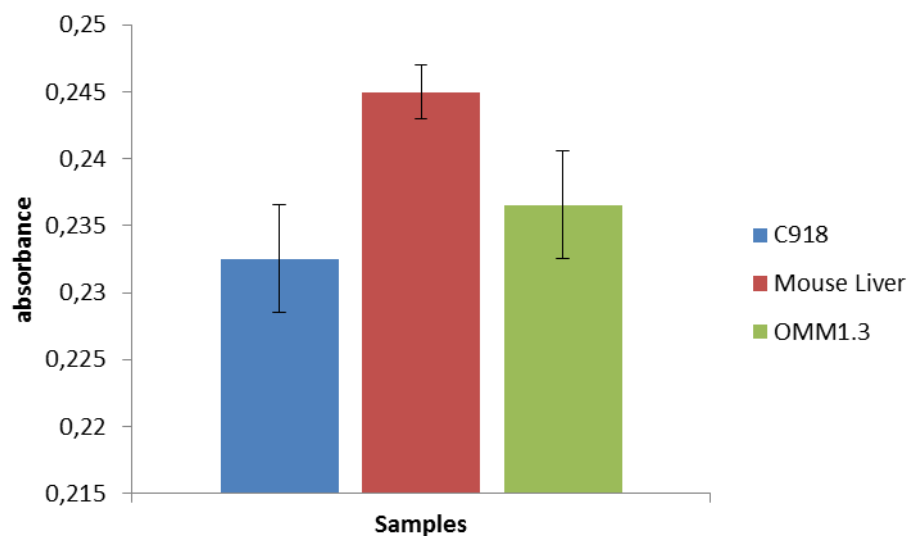


Figure S20. Detection of wt gene using modified AuNPs and total mRNA extracts (5.5 ng/ μ L) of different cell lines. C918 expresses wild type GNAQ, OMM1.3 expresses mutated GNAQ and mRNA from mouse liver that do not contain the GNAQ gene. The nanoparticles are designed to detect the wt GNAQ gene present in the C918 cell line. The drop in absorbance in the blue bar is due to the presence of the wt GNAQ gene. Values obtained as an average of three experiments

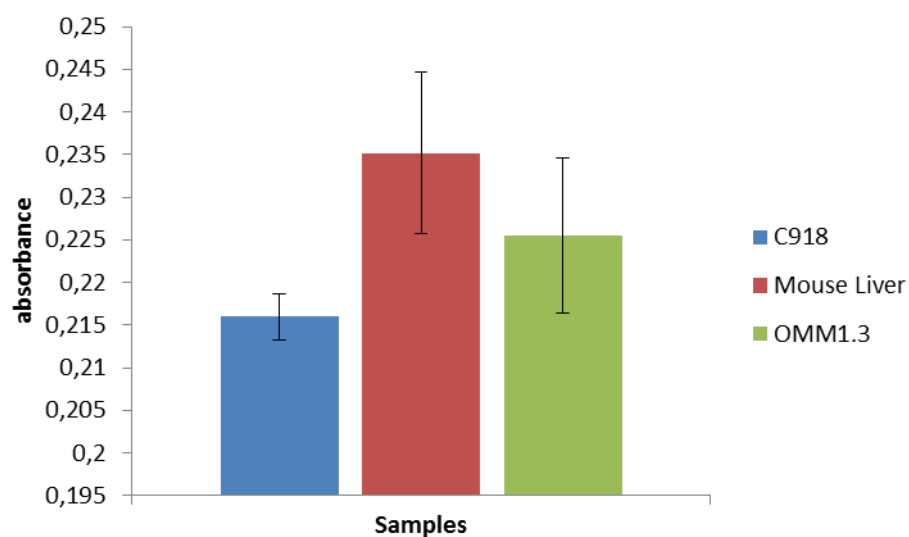


Figure S21. Detection of wt gene using modified AuNPs and total mRNA extracts (2.75 ng/ μ L) of different cell lines. C918 expresses wild type GNAQ, OMM1.3 expresses mutated GNAQ and mRNA from mouse liver that do not contain the GNAQ gene. The nanoparticles are designed to detect the wt GNAQ gene present in the C918 cell line. The drop in absorbance in the blue bar is due to the presence of the wt GNAQ gene. Values obtained as an average of three experiments

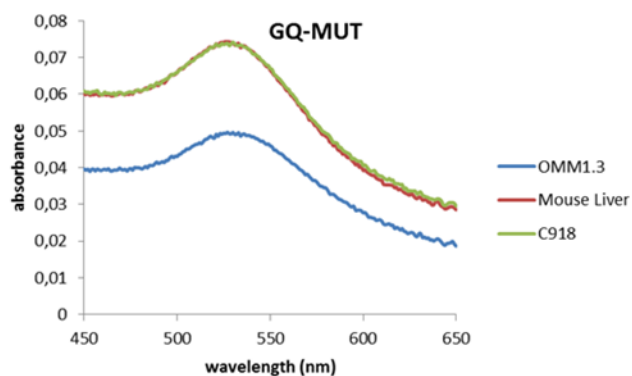


Figure S22. UV-Vis spectra of modified AuNPs after incubation with the total mRNA extracts (5.5 ng/ μ L) of different cell lines. C918 expresses wt GNAQ, OMM1.3 expresses mutated GNAQ and mRNA from mouse liver that does not express GNAQ. The nanoparticles are

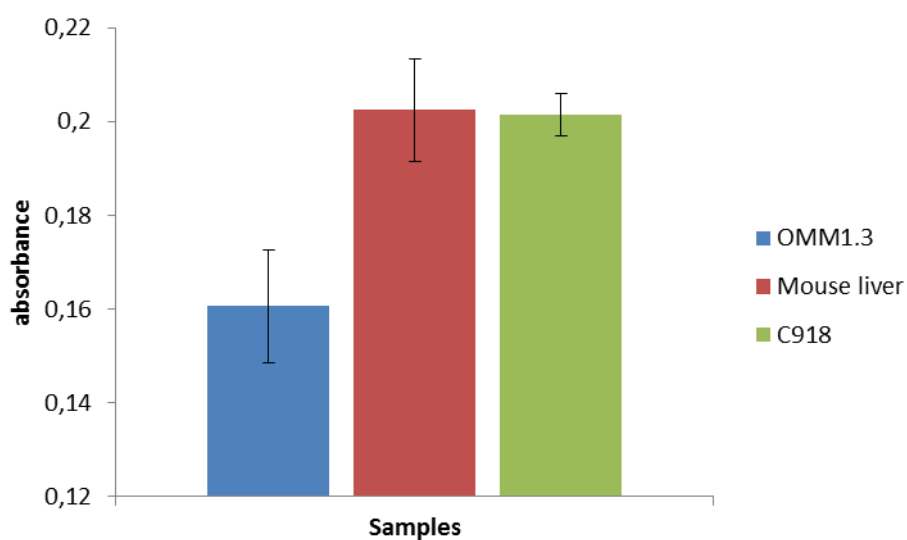


Figure S23. Detection of mutated gene using modified AuNPs and total mRNA extracts (5.5 ng/ μ L) of different cell lines. C918 expresses wild type GNAQ, OMM1.3 expresses mutated GNAQ and mRNA from mouse liver that do not contain the GNAQ gene. The nanoparticles are designed to detect the mutated GNAQ gene present in the OMM1.3 cell line. The drop in absorbance in the blue bar is due to the presence of the mutated GNAQ gene. Values obtained as an average of three experiments.

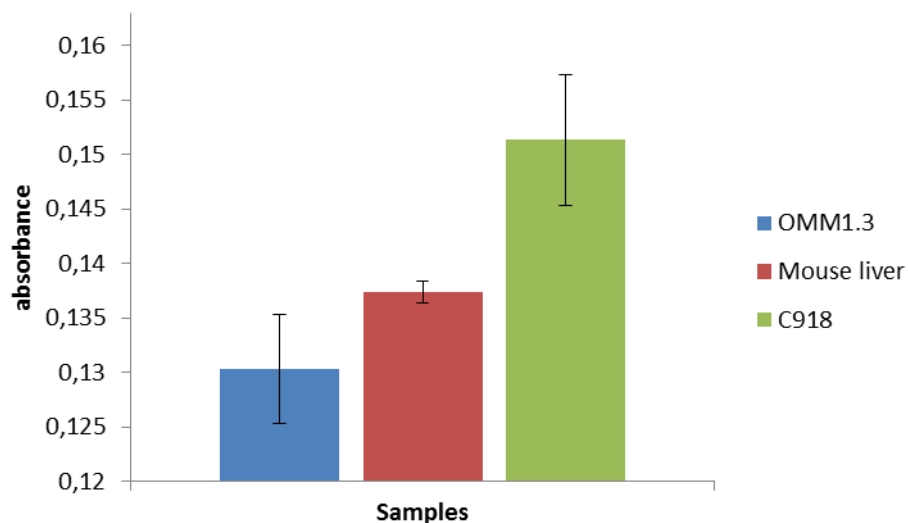


Figure S24. Detection of mutated gene using modified AuNPs and total mRNA extracts (2.75 ng/ μ L) of different cell lines. C918 expresses wild type GNAQ, OMM1.3 expresses mutated GNAQ and mRNA from mouse liver that do not contain the GNAQ gene. The nanoparticles are designed to detect the mutated GNAQ gene present in the OMM1.3 cell line. The drop in absorbance in the blue bar is due to the presence of the mutated GNAQ gene. Values obtained as an average of three experiments.

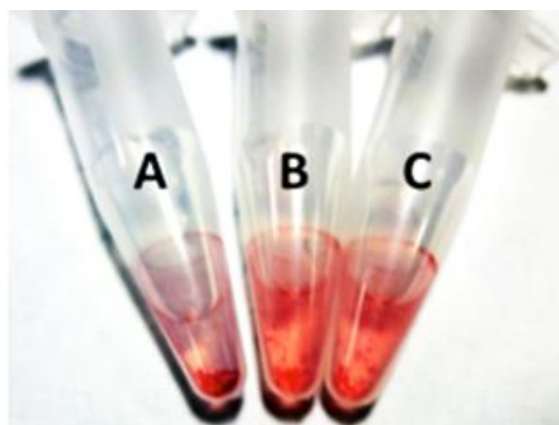


Figure S25. The AuNP sensor for mutant GNAQ allows the detection of the mutation with the naked eye. A: Extract from OMM1.3 cell line where the mutated gene is expressed. B: Extract from mouse liver where the gene is not expressed. C: Extracts from C918 cell line where the wild type gene is expressed. The total mRNA amount employed was (5.5 ng/ μ L).

Detection of mutation in the presence of a large excess of WT gene.

Gold nanoparticles (50 μL) modified with oligonucleotide 6 (designed to detect mutated GNAQ) were incubated with PBS (95 μL), NaCl (5 μL , 5M), RNA extract from OMM1.3 cell line (5 μL , 170 $\text{ng}/\mu\text{L}$) and RNA extract from C918 (5 μL , 500 $\text{ng}/\mu\text{L}$).

In the control experiment RNA extract from mouse liver (5 μL , 170 $\text{ng}/\mu\text{L}$) was used instead of OMM1.3

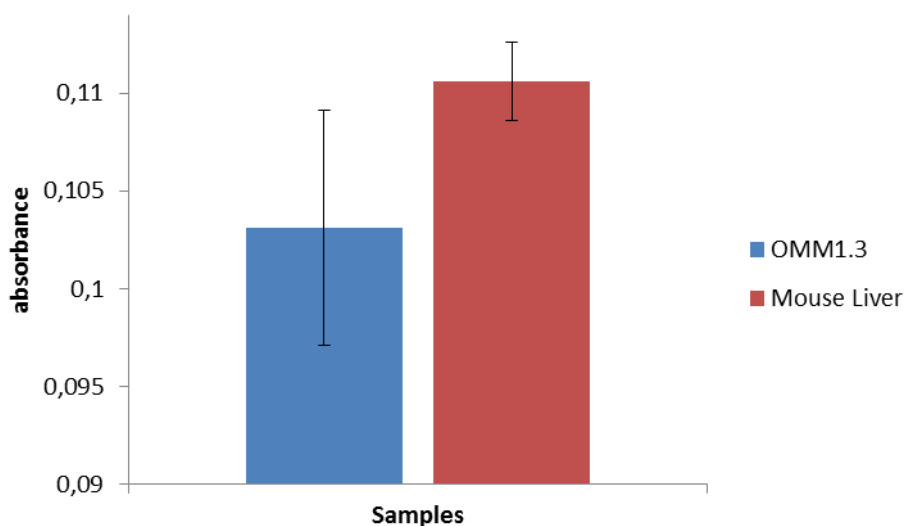


Figure S26. Detection of mutated gene in the presence of excess of WT gene. When the mutated gene is present (blue bar) there is a drop in the absorbance of gold nanoparticles at 530 nm compare with the control that has not the mutation. Both samples contain a large excess of the WT gene. Values obtained as an average of three experiments.

Hydrodynamic Size of Particles

The hydrodynamic size of the particles before and after aggregation was measured for the GNAQ-MUT system.

Hydrodynamic size was determined by dynamic light scattering (DLS) using a Zetasizer Nano (Malvern). 3 μ L of AuNPs were diluted in water (200 μ L). The measurements were performed at 25°C at a 173° scattering angle in disposable microcuvettes. The mean dynamic diameter was determined by cumulative analysis.

GNAQ-Mut particles: Z-average: 58.4 \pm 0.9634 nm ; PDI= 0.351

GNAQ-Mut particles after incubation with RNA extracts:

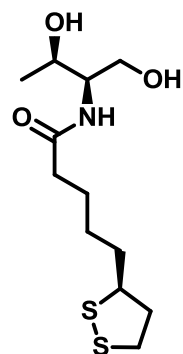
OMM1.3: Z-average: 361.1 \pm 25.37; PDI: 0.541

Mouse liver: Z-average: 323.7 \pm 12.35; PDI: 0.443

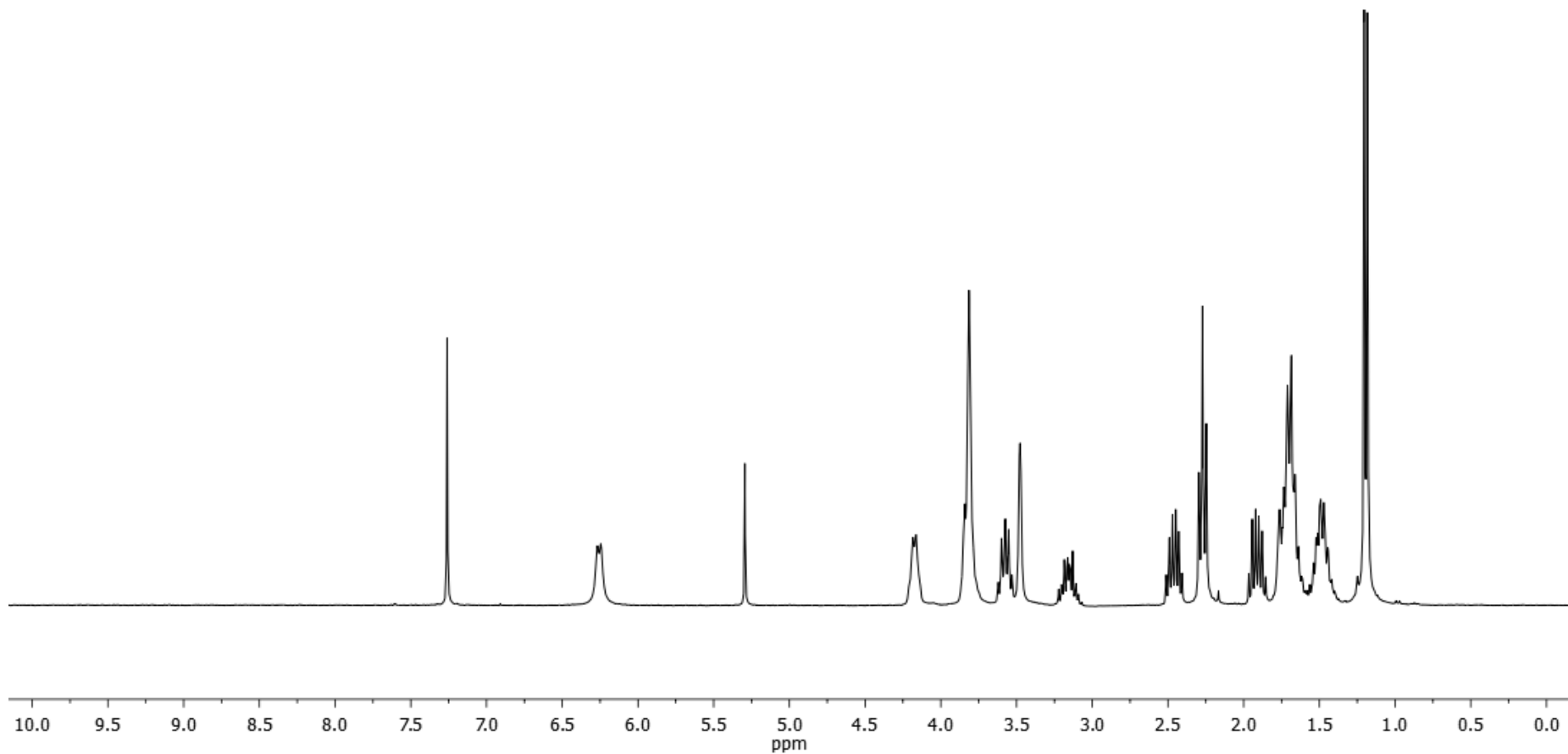
C918: Z-average: 340.2 \pm 69.19; PDI: 0.539

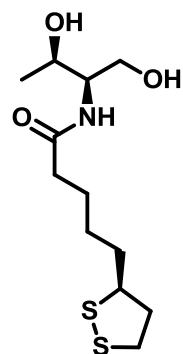
The bigger particles are present in the sample containing the mutated gene (OMM1.3). This data is in agreement with the aggregation observed and the decrease in absorbance, since the larger particles should precipitate more than the others.

NMR Spectra



1





1

